Talanta 89 (2012) 91–98

Contents lists available at SciVerse ScienceDirect

Talanta

journal homepage: www.elsevier.com/locate/talanta

Metabonomic study on the cumulative cardiotoxicity of a pirarubicin liposome powder

Wenjuan Cong[a], Qionglin Liang[b], Li Li[c], Jun Shi[d], Qingfei Liu[e], Yi Feng[a], Yiming Wang[b], Guoan Luo[b,*]

[a] Engineering Research Center of Modern Preparation Technology of TCM, Ministry of Education, Shanghai University of Traditional Chinese Medicine, Shanghai 201203, PR China
[b] Chemistry Department, Tsinghua University, Beijing 100084, PR China
[c] The Center Laboratory, Post-doctoral Research Center, The Second College of Clinical Medicine, Guangzhou University of Chinese Medicine, Guangzhou 510120, PR China
[d] School of Pharmacy, East China University of Science and Technology, Shanghai 200237, PR China
[e] School of Medicine, Tsinghua University, Beijing 100084, PR China

ARTICLE INFO

Article history:
Received 20 August 2011
Received in revised form
18 November 2011
Accepted 22 November 2011
Available online 29 November 2011

Keywords:
Pirarubicin liposome powders
Cumulative cardiotoxicity
Molecular mechanism
Metabonomics
In vitro cytotoxicity

ABSTRACT

Pirarubicin (THP) is an anthracycline frequently used in the chemotherapy against acute leukemia, malignant lymphoma and several solid tumors. However, its clinical use is severely limited by the development of a progressive dose-dependent cardiomyopathy that results in irreversible congestive heart failure. To provide a strategy for constraining or minimizing the cumulative cardiotoxicity of THP, a pirarubicin liposome powder (L-THP) was appropriately prepared, and the cumulative cardiotoxicity of L-THP and free THP (F-THP) were investigated on Sprague-Dawley rats after 3 successive doses. Urinary samples for metabonomic study, serum samples for biochemical assay, and heart samples for histopathology test were collected. As a result, the metabonomics-based findings such as PLS-DA plotting showed minimal metabolic alterations in L-THP as compared to F-THP, and correlated with the changes of serum biochemical assay and cardiac histopathology as measurements of damage to heart tissue. Our results confirm that when encapsulated into liposomes, the cumulative cardiotoxicity of THP can be greatly ameliorated. Lipophilic aglycone metabolites of THP associated with redox cycling are cardiotoxic for the possibility of reactive oxygen species (ROS) formation. Also, metabonomic analysis shows that the successive doses of THP will lead to severe metabolic pathways disturbances in the cell energy production. Further, the preliminary efficacy study of L-THP on lung cancer was evaluated in the approach of *in vitro* cytotoxicity on A549 cells by high content screening (HCS) analysis, and L-THP was found to exhibit better therapeutic index against lung cancer than THP.

1. Introduction

Anthracyclines, notably doxorubicin (DOX), epirubicin and daunorubicin, are potent antineoplastic agents used extensively to treat a range of cancers, including leukemias, lymphomas, sarcomas and carcinomas [1–4]. However, the clinical use of anthracyclines can be reviewed as a sort of double-edged sword. On the one hand, they can play an undisputed key role in the cancer therapy; on the other hand, their successive doses will induce irreversible cardiomyopathy that can be lethal even after the cessation of treatment [5]. Pirarubicin (THP) (Fig. 1), a-tetrahydropyranyl (DOX), is often used in the chemotherapy against acute leukemia, malignant lymphoma and several solid tumors. Although THP has been frequently reported to exhibit satisfactory cardiotoxicity at a single dose in the anthracycline family [6,7], there is still a risk of cardiomyopathy at cumulative doses. For instance, THP causes a significant decrease in the left ventricular ejection fraction at a cumulative dose of 460 mg/m^2 or can lead to full-blown congestive heart failure (CHF) at greater than 500 mg/m^2 for women with metastatic breast cancer [8]. Also, THP can cause severe cardiac dysfunction at a cumulative dose of 360 mg/m^2 for elderly patients with non-Hodgkin's lymphoma [9]. In addition, dilative cardiomyopathy and CHF can develop after the completion of cumulative THP regiments [5]. Therefore, there is a need to identify ways to prevent or alleviate the cumulative cardiotoxicity of THP in order to improve its therapeutic index.

A liposomal drug delivery system, a proven strategy for constraining or preventing anthracycline-induced cardiotoxicity [10,11], can alter the *in vivo* behavior, alleviate the severe side effects and thus improving the therapeutic index of the encapsulated drug [12,13]. Pharmacokinetic studies have shown that the heart accumulation of THP can be greatly reduced after a single dose when encapsulated into liposomes [14,15]. However, no studies to date are concerned to the assessment of cumulative cardiotoxicity of pirarubicin liposomes (L-THP). In addition, the

* Corresponding author at: Department of Chemistry, Tsinghua University, Haidian District, Beijing 100084, PR China. Tel.: +86 10 62781688; fax: +86 10 62781688.
E-mail address: luoga@tsinghua.edu.cn (G. Luo).

0039-9140/$ – see front matter.
doi:10.1016/j.talanta.2011.11.071

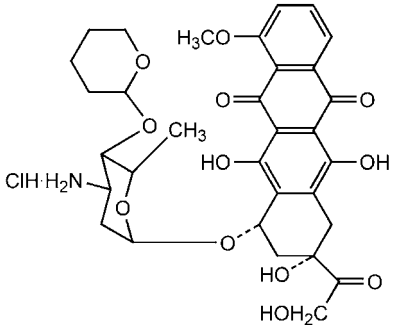

Fig. 1. The molecular structure of pirarubicin.

pathophysiology of THP induced cardiomyopathy remains controversial and the pharmacological impacts on the global metabolism and histopathology upon the successive doses are still incompletely understood.

Metabonomic approaches, the multicomponent analysis of the biochemical composition of body fluids combined with statistical models, are increasingly being used in drug and chemical safety assessment to diagnose or predict toxicity [16–18]. As a high throughput "omic" approach, it can well reveal the pathophysiological perturbations of the diseases through searching for disease-related potential biomarkers and metabolic pathway [19–21]. The principal analytical technique for global metabolic profiling has long been hyphenated liquid chromatography–mass spectrometry (LC–MS) technology. Due to the reproducibility enhancement of retention time, ultra-performance liquid chromatography/mass spectrometry (UPLC/MS) is considered as a robust tool in the metabonomic study [22,23]. Similarly, multiparametric analysis of compound toxicity at the level of individual cells using flow cytometry and cellular imaging-based approaches, such as high-content screening (HCS), have played key roles in the detection of toxicity and classification of compounds based on the observed patterns of reversible and irreversible cellular injuries [24,25].

In this paper, we performed a urine metabonomic study based on UPLC/TOF–MS, coupled with the analysis of serum biochemical indices and heart histopathology, for the assessment of cumulative cardiotoxicity in Sprague-Dawley rats after successive doses of L-THP and F-THP. In addition, we also reported an *in vitro* study comparing the effect of L-THP and F-THP on A549 lung cells as an indicator of the effect of liposomal encapsulation of THP on its potential cytotoxicity. We want to explore comprehensive metabolic information for pathological variations of L-THP and F-THP, and the important molecular mechanism associated with cumulative cardiotoxicity of THP.

2. Materials and methods

2.1. Materials

0.9% physiological saline was purchased from Double-crane Pharmaceutical Co., Ltd. (Beijing, China) and pirarubicin hydrochloride (THP, 99.5% purity) was purchased from Shenzhen Olympic Star Pharmaceutical Co., Ltd. (Guangdong, China). Pirarubicin hydrochloride powder for injection (F-THP) was obtained from Shenzhen Main Luck Pharmaceuticals Inc. (Guangdong, China). The assay kits for lactate dehydrogenase (LDH) and creatine kinase (CK) for serum biochemical test were purchased from Nanjing Jiancheng Bio-engineering Institute (Nanjing, China). Formalin, hematoxylin–eosin and hydrogen peroxide solution for the histopathology test were from Beijing Yili Fine Chemicals Co., Ltd. (Beijing, China). Acetonitrile and methanol used for UPLC/TOF–MS analysis were of HPLC grade, and were purchased from J.T. Baker (Phillipsburg, NJ, USA). Formic acid, leucine enkephalin, citrate, α-D-glucuronic acid 1-phosphate tripotassium salt pentahydrate, N-acetyl-DL-tryptophan, N-acetyl-L-glutamine, L-lactic acid sodium salt, uridine and PA(18:1(9Z)/18:1(9Z)) were obtained from Sigma–Aldrich (St. Louis, MO, USA). Ultrapure water (18.2 MΩ cm) was prepared with a Milli-Q water purification system (Millipore, France). All cell culture and HCA reagents were obtained from Invitrogen Corporation (CA, USA). A549 cells were a gift from the Biology Department of Tsinghua University (Beijing, China).

2.2. Animals and treatment

Male Sprague-Dawley rats (250 g ± 10 g) were purchased from Beijing Weitong Lihua Experimental Animals Co., Ltd. (Beijing, China), individually housed in humidity and temperature controlled rooms with a 12-h light/dark cycle. Animals were allowed free access to standard laboratory chow and water, and acclimated for 1 week prior to dosing. The animal facilities and protocols were approved by the Institutional Animal Care and Use Committee, Tsinghua University. All procedures were in accordance with the National Institute of Heath's guidelines regarding the principles of animal care (2004).

Rats were randomized by weight and divided into drug-treated groups (F-THP or L-THP) and untreated groups (blank liposomes or control) ($n = 7$ or 8 animals per group). L-THP and blank liposome powder were appropriately prepared as previously described [14], and solutions of L-THP, F-THP and blank liposomes were prepared with sterile water for dosing. Drug-treated groups were intravenously injected at a dosage of 14 mg THP/kg, whereas untreated groups received an equal volume of blank liposomes and 0.9% physiological saline, respectively. Animals were dosed on the 1st, 3rd and 5th day with a 48-h interval, and sacrificed by decapitation on day 6. Bodyweight as well as food and water consumption were recorded daily. Urine was collected at a 24-h interval after each dosing, and kept at −80 °C for UPLC/TOF–MS analysis. Blood samples were drawn from the ocular orbit of rats on day 6 prior to sacrifice, and serum was obtained for preclinical biochemistry analysis. Heart tissues were collected immediately after sacrifice, weighed, fixed into neutral buffered formalin for histopathology analysis.

2.3. Histopathology test

Heart samples were dehydrated using Leica TP 1020 dedroextractor (Leica Microsystems Ltd., Hongkong, China), steeped and embedded in paraffin wax. Histological sections, about 4–5 μm, were stained with hematoxylin–eosin. Sections were then examined under Nikon 55i Microscope (Nikon Instruments Inc., Tokyo, Japan), and photomicrographs were taken using HMIAS-2000 high definition and colorful image analytical system (magnification 100×) (Qianping Image Co., Wuhan, China).

2.4. Preclinical chemical assay

Creatine kinase (CK) and lactate dehydrogenase (LDH) in serum were analyzed immediately on a Roche Hitachi 917 instrument (Roche Diagnostics, Inc., Indianapolis, IN) using standard protocols according to the manufacturer's instructions.

2.5. UPLC/TOF–MS analysis.

Thawed urine samples (100 μL) were mixed with methanol (400 μL) by vortex for 2 min, and centrifuged at 4 °C for 15 min at 13,000 rpm. The resulting supernatant was transferred to a 1.5 mL polypropylene tube, diluted with 500 μL of ultrapure water, and filtered through a syringe filter (0.22 μm) for UPLC/TOF–MS analysis.

Chromatographic separation was performed using a Waters ACQUITY UPLC system equipped with a binary solvent delivery system, a PDA detector and an autosampler (Waters Corporation, Milford, USA). A BEH C_{18} column (2.1 mm × 100 mm, 1.7 μm) (Waters Corporation, Milford, USA) was used, maintained at 50 °C with a flow rate of 0.4 mL/min. The mobile phase was composed of phase A (water with 0.1% formic acid (by volume)) and phase B (acetonitrile), and the optimized gradient program was as follows: 0–5 min, 5–50% B; 5–6 min, 50–95% B; 6–7 min, 95% B; 7–8 min, 95–5% B; 8–11 min, equilibrated with 5% B. The column was then directed to the mass spectrometer without split.

Mass spectrometry was performed on a Waters LCT Premier orthogonal accelerated time of flight mass spectrometer (Waters Corporation, Manchester, UK) with an electrospray ionization source (ESI) operating in a negative ion mode (W mode of operation). The capillary voltage was set at 2300 V and cone voltage was 35 V. Nitrogen was used as the dry gas and the desolvation gas flow rate was set to 600 L/h at a temperature of 350 °C. Cone gas flow was maintained at 40 L/h and the source temperature was set at 120 °C. The scan time and inter-scan delay were set to 0.1 s and 0.02 s, respectively. All the analyses were acquired using an independent reference lock mass ion via the LockSpray™ interface to ensure its accuracy and reproducibility. Leucine enkephalin was used as the reference compound ($[M-H]^-$ = 554.2615) at a concentration of 50 pg/μL under a flow rate of 10 μL/min. The data were collected in the centroid mode from m/z 50 to m/z 1500 with a LockSpray frequency of 10 s and averaged over 10 scans for correction.

The obtained MS data were collapsed into a single matrix by aligning peaks with the retention time-exact mass pair together along with the associated intensities using Markerlynx Applications Manager version 4.1 (Waters, Manchester, UK), which incorporates a package allowing the detection and retention time alignment of the peaks in each chromatogram [26]. The major parameters for data processing were set as follows: retention time (0–11 min), mass range (50–1000 Da), mass tolerance (0.02 Da), minimum intensity (15% of base peak intensity), maximum mass per retention time (6) and retention time tolerance (0.02 min). Prior to multivariate statistical analysis, the exclusion of noise and background interference, and normalization of the total sum of the chromatogram were performed [27]. The resulting data set was then imported into SIMCA-P 11.5 software package (Umetrics, Umeå, Sweden). The data was mean-centered and pareto-scaled prior to multivariate statistical analysis.

Unsupervised principle component analysis (PCA) was initially used to detect intrinsic clustering and obvious outliers within the sample set. To visualize the maximal difference of global metabolic profiles between treatment groups (F-THP, L-THP or blank liposomes) and control group, a supervised discriminant technique, partial least squares-discriminant analysis (PLS-DA) was carried out. For PCA and PLS-DA modeling in the SIMCA-P+ software, the components necessary for modeling were automatically calculated by the software. A default 7-round cross-validation was applied to guard against overfitting, with 1/7th of the samples being excluded from the mathematical model in each round. Also, a 999 random permutations test also performed to further validate the supervised model. The values of parameters (R^2Y and Q^2Y) indicate the predictability of a mathematical model, and $Q^2Y \geq 0.4$ is generally considered a reliable model [28]. The variable importance in the projection (VIP) values of all the peaks from 7-fold cross-validated PLS-DA model were taken as a coefficient for peak selection. VIP ranks the overall contribution of each variable to the PLS-DA model, and those variables with VIP > 1.0 were considered relevant for group discrimination [29]. In parallel, one univariate method, the Student's test, was selected to measure the significance of each metabolite in separating THP from controls ($p < 0.05$). Then several peaks responsible for the differentiation of the metabolic profiles of THP-treated groups and untreated groups could be obtained by comprehensive consideration of these two coefficients.

Table 1
CK and LDH assay in the rat serum for different groups after 3 successive administrations (mean ± SD).

Group	CK/μmol mL^{-1}	LDH/μmol mL^{-1}
Control (n = 7)	1.657 ± 0.252	19.196 ± 4.415
Blank liposomes (n = 8)	2.543 ± 0.751	14.314 ± 4.050
L-THP (n = 8)	2.007 ± 0.504*,**	13.275 ± 4.559*
F-THP (n = 7)	3.832 ± 1.604*	18.588 ± 3.942

* $p < 0.05$ *vs.* control group.
** $p < 0.05$ *vs.* F-THP.

2.6. In vitro cytotoxicity of L-THP and F-THP against A549 cells

As our previous study showed that both L-THP and F-THP were accumulated in the lung tissue [14], the effect of L-THP and F-THP were investigated in A549 lung cancer cells. Prior to counting and plating, cells were mixed vigorously and gently passed through a $26_{5/8}$ – gauge needle and a 40-μm nylon cell strainer from BD Bioscience to minimize cell clumping. Cells were plated at a density of 3000 cells/100 μL in 96-well collagen I coated microplates, and then cultured overnight. Due to the evaporation-related edge effects in the outside wells, only the inner 60 wells of 96-well microplates were used. Tacrine, has widely reported effects on mitochondrial function, plasma membrane permeability, nuclear morphology and cell proliferation [25], was used as a control compound. After a 24 h incubation, L-THP or F-THP testing solutions containing a THP concentration of 200 μg/mL, 20 μg/mL, 2 μg/mL and 0.2 μg/mL were made. The cell permeable dye Hoechst 33342, live cell impermeable DNA binding dye YOYO-1 and MitoTracker Red dye were used to measure nuclear morphology, plasma membrane integrity and mitochondrial function, respectively.

The assay plate was imaged and analyzed using the Cell Health Profiling BioApplication on the ArrayScan® VTI HCS Reader (Thermo Fisher Scientific-Cellomics, Pittsburgh, PA) using the 10× objective [30]. Statistical analysis was performed using Microsoft Excel 2003 Analysis Tool Pack and S-Plus 2000 (MathSoft Inc., Seattle, WA). Statistical differences of the mean values for various parameters among the groups were tested using the two-sided Student's t-test with α set to 0.01. A p value <0.01 was considered statistically significant.

3. Results

3.1. Effect of successive doses on the preclinical biochemical assay

The standard serum clinical markers CK and LDH were measured in the drug-treated rats. These were also detected in all the untreated rats, enabling a comparison of fold changes among each group (Table 1). Both L-THP and F-THP induced increases in CK, although the L-THP induction was significantly less than F-THP ($p < 0.05$). However, in this study, changes in LDH were variable and showed no significant either L-THP or F-THP compared to controls.

3.2. Effect of successive doses on the histopathology test of heart samples

A histopathological analysis of heart showed that rats dosed with either saline or blank liposomes, the myocardial cells were characterized by closely ordered muscle bundles arranged longitudinally in a regular pattern and with rod-shaped nuclei (Fig. 2A and B, respectively). L-THP treatment showed some disordered arrangement of myocardial cells and the presence of inflammatory cells (Fig. 2D). However, F-THP caused a severe disruption

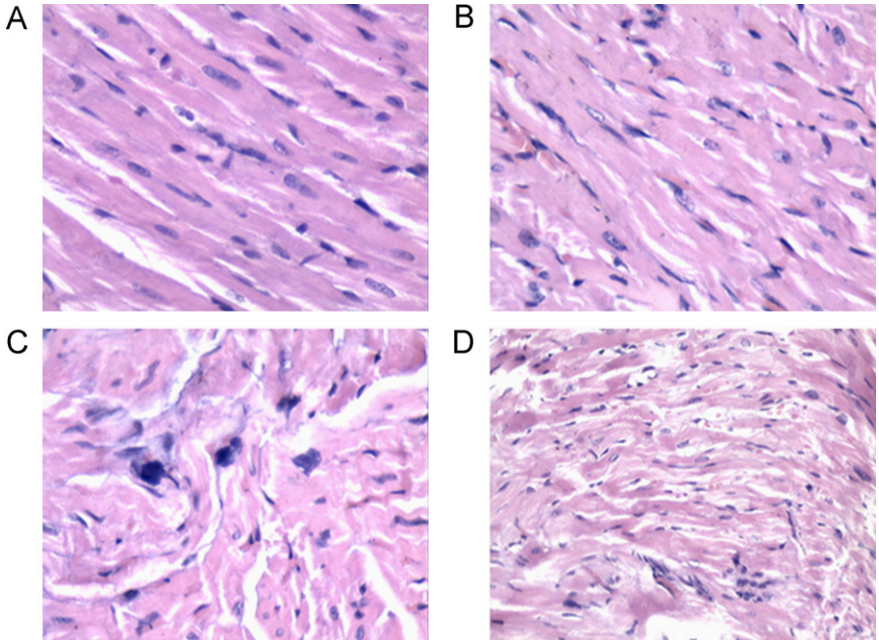

Fig. 2. Histopathological observations of heart tissues for different treatments after 3 successive dosing (magnification 400 diameters) (A: H–E staining microscope photograph of rats dosed with saline; B: H–E staining microscope photograph of rats dosed with blank liposomes; C: H–E staining microscope photograph of rats dosed with F-THP; D: H–E staining microscope photograph of rats dosed with L-THP).

of the longitudinal arrangement of the myocardial cells, myofiber degeneration, myonecrosis and cellular infiltrates (Fig. 2C).

The adverse effects of THP after successive doses on serum biochemistry and heart histopathology are consistent with overt toxicity of THP treatment as measured by a statistically significant body weight reduction of rats compared to control animals ($p < 0.05$, data not shown).

3.3. *Effect of successive doses on the urine metabolic profiling based on UPLC/TOF–MS analysis*

In our preinvestigation study, the urine metabolic fingerprints had been fully optimized after careful optimization of the operation mode of electrospray ionization source (ESI), capillary voltage, flow and temperature of desolvation gas for the mass spectrometry detector, and the flow rate and column temperature for the chromatography (see in Section 2.5). Also, we made a study on the urine extraction protocol. And we found that direct diluting method would easily cause protein "plug", thus greatly affecting the chromatography; the addition of methanol could avoid this phenomena. The urine extraction protocol in this paper, was untargeted as well as a conventional use in the discovery metabonomics [26,27]. It may not be indeed the best strategy in our metabonomic study and some metabolites may be lost. However, these lost of each sample could be parallel as the process was controlled strictly in the experiment and the result of methodology validation showed the repeatability was acceptable.

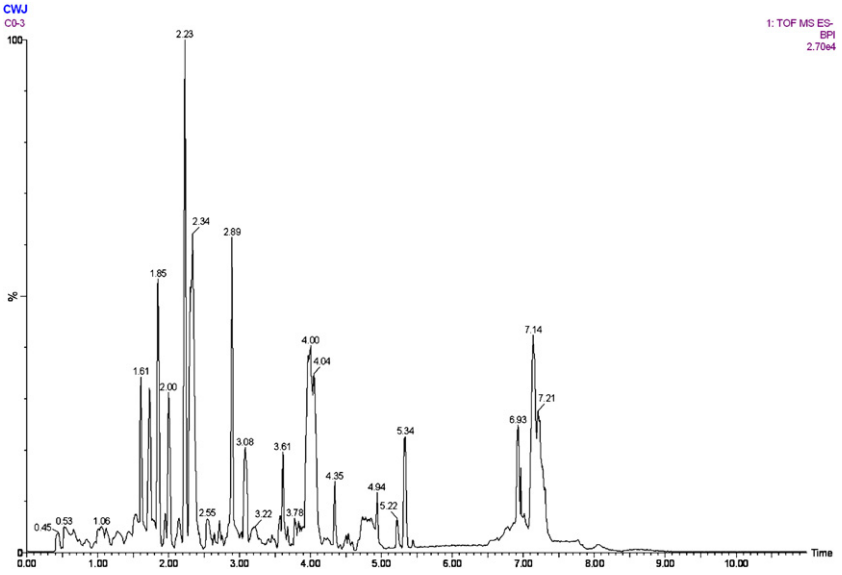

Fig. 3. Representative base peak intensity chromatogram of the rat urine obtained in ESI negative mode based on UPLC/TOF–MS.

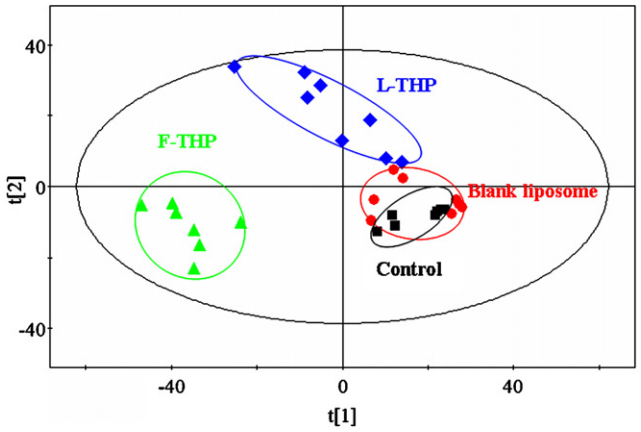

Fig. 4. PLS-DA score plots of rat urine data of different groups ($n = 7$). (Symbols of (■) represented the data from rats dosed with saline; and (●) were the data from rats dosed with blank liposomes; (♦) were the data from rats dosed with L-THP; (▲) were the data from rats dosed with F-THP.)

After the optimization of experiment conditions, a representative base peak intensity chromatogram of the rat urine (Fig. 3) was obtained. Subsequently, the precision and reproducibility of the UPLC/MS method were validated by the reduplicate analysis of 6 parallel samples prepared using the same preparation protocol. The relative standard derivations of the retention time and peak intensity for the main peaks were less than 5.0%, indicating that the precision and reproducibility of sample preparation met the requirements for the metabonomic analysis.

PCA and PLS-DA are useful to reveal the pathophysiological perturbations of different groups [23]. In this test, PCA was firstly performed to differentiate distinct urinary metabolite profiles of all treatments, and PLS-DA was subsequently constructed to identify the metabolites contributing to the separation of the metabolic patterns of different treatments. The PLS-DA score plot (Fig. 4) ($R^2X = 0.527$, $R^2Y = 0.985$, $Q^2Y = 0.772$) shows that the trajectories of the L-THP-treated group is in closer proximity to the saline treated group. This suggests that the metabolic changes occurring during L-THP treatment are minimal. In contrast, the F-THP treated group is the most distal reflecting the greatest global metabolic alterations happened after the successive doses. These metabonomic alterations are in good agreement with histopathology observations of cardiac tissue following these treatments (see Fig. 3).

On the basis of a VIP threshold of 1 from the 7-fold cross-validated PLS-DA model, a number of metabolites responsible for the discrimination in the metabolic profiles of different treatments could be obtained. In parallel, the metabolites identified by PLS-DA model were validated using Student's test. The critical p-value was set to 0.05 for significantly differential variables in this study. Following the criterion above, 15 metabolites (listed in Table 2) were selected for further study.

The identity of 7 metabolites, namely D-gluconate-1-phosphate, N-acetylglutamine, citrate, lactate, uridine, N-acetyl-DL-tryptophan and PA(18:1(9Z)/18:1(9Z) were confirmed using authentic standards. 4 other metabolites were identified as oxidation, hydrolysis and reduction products of THP by comparison with the known metabolic profile of DOX [31]. In this way, adriamycinone, 7-deoxyadriamycinone, 13-dihydroadriamycinone and 7-deoxy-13-dihydroadriamycinone were identified as metabolites of THP by matching their retention time and accurate mass measurement with available reference standards [32–34]. Adriamycinone and 7-deoxyadriamycinone result from hydrolytic or reductive deglycosidation of THP, and were then transformed to 13-dihydroadriamycinone and 7-deoxy-13-dihydroadriamycinone through two-electron reduction in the medium of cytosolic reductases (Fig. 5). The identification of pantetheine 4′-phosphate, deoxycholic acid 3-glucuronide, urobilinogen was made by searching freely accessible databases (http://www.genome.jp; http://www.hmdb.ca) utilizing detected molecular weights and elemental compositions.

We casually selected 9 metabolites as the "potential biomarkers" (listed in Table 3) based on the certainty of their identity, and the measurable changes in their peak intensity for different treatments were also summarized (listed in Table 3). It was noted that there was an increased expression of THP metabolites, although there was no significant difference between L-THP and F-THP. Interestingly, we found that some metabolites were involved in the metabolic process related to myocardial energy metabolism, including tricarboxylic acid (TCA) cycle (citrate), glycosis (lactate), pentose phosphate pathway (D-gluconate-1-phosphate) and amino acid metabolism (N-acetylglutamine and N-acetyl-DL-tryptophan). These metabolites were significantly down-regulated in the drug treatment groups. Furthermore, F-THP treatment resulted in a greater down regulation of intermediary metabolites compared to L-THP treatment.

Table 2
Identification of significantly differential metabolites in the rat urine.

No.	R.T. (min)	m/z	Selected ion	Elemental composition	Identification results	Blank liposomes[c]	L-THP[c]	F-THP[c]
1	2.34	461.1817	$[M+HCOO]^-$	$C_{21}H_{20}O_9$	13-Dihydroadriamycinone[b]	–	+(↑)	+(↑)
2	2.27	459.1985	$[M+HCOO]^-$	$C_{21}H_{18}O_9$	Adriamycinone[b]	–	+(↑)	+(↑)
3	2.56	443.1727	$[M+HCOO]^-$	$C_{21}H_{18}O_8$	7-Deoxyadriamycinone[b]	–	+(↑)	+(↑)
4	2.15	445.1884	$[M+HCOO]^-$	$C_{21}H_{20}O_8$	7-Deoxy-13-Dihydroadriamycinone[b]	–	+(↑)	+(↑)
5	2.89	595.2006	$[M-H]^-$	$C_{36}H_{40}N_2O_6$	Urobilinogen[b]	–	+(↑)	+(↑)
6	1.73	357.1062	$[M-H]^-$	$C_{11}H_{23}N_2O_7PS$	Pantetheine 4′-phosphate[b]	–	+(↑)	+(↑)
7	2.00	385.1377			Unknown	+(↓)	+(↑)	+(↑)
8	4.93	699.483	$[M-H]^-$	$C_{39}H_{73}O_8P$	PA(18:1(9Z)/18:1(9Z))[a]	+(↑)	+(↑)	+(↓)
9	2.22	567.1695	$[M-H]^-$	$C_{30}H_{48}O_{10}$	Deoxycholic acid 3-glucuronide[b]	–	+(↑)	+(↑)
10	0.57	191.0089	$[M-H]^-$	$C_6H_8O_7$	Citrate[a]	–	+(↓)	+(↓)
11	1.53	272.9992	$[M-H]^-$	$C_6H_{11}O_{10}P$	D-gluconate-1-phosphate[a]	–	+(↓)	+(↓)
12	1.72	187.0909	$[M-H]^-$	$C_7H_{12}N_2O_4$	N-acetylglutamine[a]	–	+(↓)	+(↓)
13	1.70	242.9905	$[M-H]^-$	$C_9H_{12}N_2O_6$	Uridine[a]	–	+(↓)	+(↓)
14	1.61	245.0034	$[M-H]^-$	$C_{13}H_{14}NO_3$	N-acetyl-DL-tryptophan[a]	–	+(↓)	+(↓)
15	0.62	89.0228	$[M-H]^-$	$C_3H_6O_3$	Lactate[a]	–	+(↓)	+(↓)

All data represent the intensity values of metabolites on day 6. The upward arrow (↑) means significantly elevated concentrations, whereas the downward arrow (↓) represents significantly lowered concentration.

[a] Compounds confirmed with authentic standards.

[b] Compounds identified by accurate mass measurement ($p < 0.05$).

[c] Compared to the normal controls, "+" means statistical significant difference and "–" means no statistical significant difference.

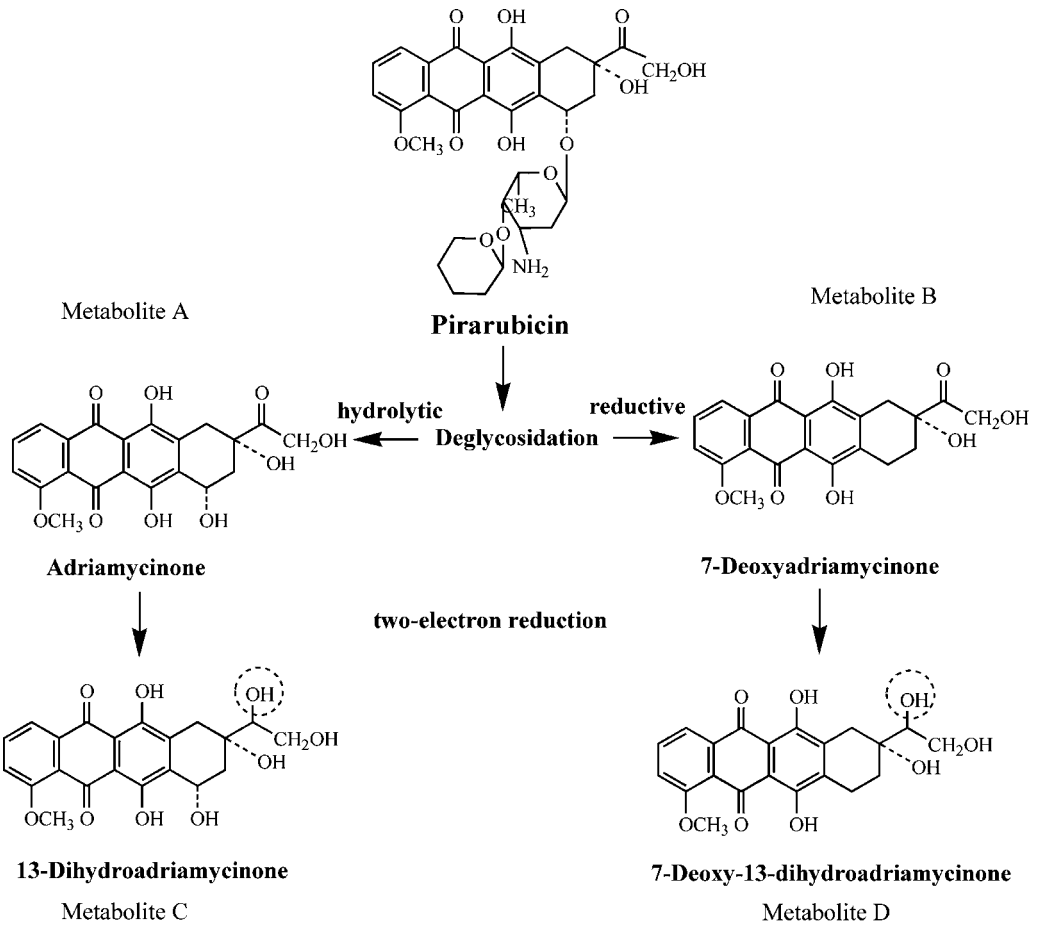

Fig. 5. Scheme showing THP metabolites and possible routes of transformation.

Table 3
Summary of intensity values of potential biomarkers in each group on day 6.

Biomarkers	Peak intensity (Mean ± SD)			
	Control (n = 7)	Blank liposomes (n = 8)	L-THP (n = 8)	F-THP (n = 7)
13-Dihydroadriamycinone	1.12 ± 0.23	1.86 ± 0.29	281.84 ± 78.63*	312.45 ± 60.82*
Adriamycinone	0.25 ± 0.21	0.32 ± 0.13	10.61 ± 1.92*	7.41 ± 1.30*
7-Deoxyadriamycinone	0.87 ± 1.09	1.51 ± 0.60	69.70 ± 16.82*	58.20 ± 20.56*
7-Deoxy-13-dihydroadriamycinone	1.21 ± 1.07	0.69 ± 0.14	73.75 ± 17.04*	53.50 ± 6.18*
D-gluconate-1-phosphate	114.06 ± 21.57	92.65 ± 23.45*	65.20 ± 15.16*	27.90 ± 4.99*,**
Citrate	56.60 ± 11.84	62.16 ± 11.92	45.65 ± 5.95*	20.45 ± 3.58*,**
N-acetylglutamine	40.15 ± 4.68	40.46 ± 5.27	32.35 ± 4.53	18.70 ± 2.25*,**
N-acetyl-DL-tryptophan	63.36 ± 13.59	65.67 ± 10.67	43.10 ± 6.67*	23.32 ± 4.22*,**
lactate	10.45 ± 1.33	11.06 ± 1.20	7.78 ± 1.21	1.29 ± 1.20*,**

* $p < 0.05$ *vs.* control group.
** $p < 0.05$ *vs.* L-THP.

3.4. *In vitro cytotoxicity results of F-THP and L-THP against A549 cells*

Nuclear morphology, mitochondrial membrane potential (MMP) and plasma membrane permeability (PMP) as indicators of toxicity [35]. Untreated, F-THP and L-THP treated A549 cells were analyzed using a high content screening process (Fig. 6). The results show a dose-dependent toxicity as indicated by significant changes ($p < 0.05$) in PMP, MMP and nuclear swelling and fragmentation for both L-THP and THP treatments. Generally, L-THP was more cell damaging than free THP ($p < 0.05$), suggesting that the liposomal preparation enhances THP delivery and attendant toxicity to the A549 cells.

4. Discussions

It is established that, as a colloidal drug delivery system, liposomes can modulate the *in vivo* behavior of the entrapped drug in the hydrophobic core, thus lowering the drug-related toxicity and improving the therapeutic index of drugs [36]. Our previous pharmacokinetic study showed that the heart accumulation of THP could be significantly reduced after single dose when encapsulated into liposomes [14]. However, few literatures are concerned to the assessment of cumulative cardiotoxicity of THP and the pharmacological impacts on the global metabolism and histopathology upon the successive doses. Therefore, the present study was designed to investigate the effect of successive doses of THP on its

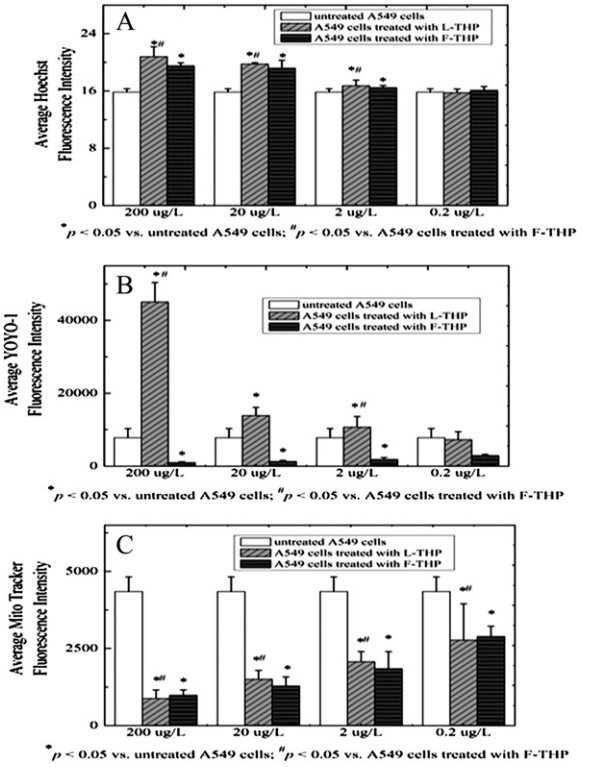

Fig. 6. The effects of L-THP and F-THP on nulcear morphology (A), plasma membrane permeability (B) and mitochondrial membrane potential (C) (data reported are mean ± SD, $n = 6$).

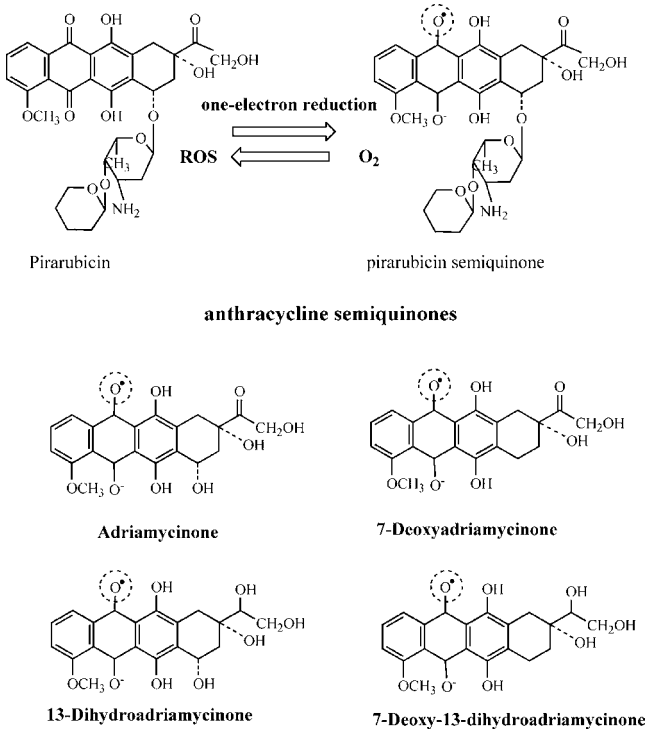

Fig. 7. Proposed mechanism of reactive oxygen mediated cardiotoxicity induced by THP and its metabolites.
Adapted from Ref. [31].

cumulative cardiotoxicity via metabonomic analysis coupled with serum biochemical and histopathology test. We aimed to further define the toxicity profiles of L-THP and F-THP with a view to identifying biomarkers of cardiotoxicity for use in drug development and to assess their potential as biomarkers for clinical application.

Myocardial injuries dramatically alters energy metabolism, leads to the cell homeostasis disruption, and thus resulting an increased CK and LDH levels [26,36]. In this study, a significant and rapid increase of CK following successive THP dosing was shown, and is consistent with accumulative myocardial injury. However, LDH did not increase with either F-THP or L-THP treatments despite its published use as a biomarker of injury [26]. The THP dose used in this study may not be sufficient to elicit an elevation of LDH.

Histopathology results of heart tissue showed that THP-treatment does result in serious irreversible myocardial injury after 3 successive doses, but interestingly, this can be alleviated when encapsulated into the liposomes. The use of liposomal drug delivery system is particularly important given the irreversibility of myocyte damage of THP. The absence of adverse affects in the blank liposome treatment is consistent with the known safety of this vehicle, and specifically is shown safe to myocardial cells *in vivo*.

Potential biomarkers, such as adriamycinone, 7-deoxyadriamycinone, 13-dihydroadriamycinone and 7-deoxy-13-dihydroadriamycinone, are the aglycones of THP. It is noted that one electron reduction of the quinone moiety in C ring of anthracyclines will result in the formation of a semiquinone radical. This will undergo facile redox cycling in the oxygenated tissues including the heart to regenerate the parent quinone concomitant with the formation of the superoxide anion ($O_2^{\bullet -}$) and its dismution product hydrogen peroxide (H_2O_2) (Fig. 7). Hence, the anthracyline family of antitumour antibiotics are widely reported to increase the reactive oxygen species (ROS) concentration over the physiologic levels generated during the normal aerobic metabolism. Due to their lipophilicity, anthracycline aglycones can readily intercalate into the mitochondrial membranes, and are believed to generate mitochondrial damaging ROS species [37,38]. In addition, these metabolites can induce mitochondrial dysfunction, energy imbalance, disruption of the cardiac specific gene expression program and apoptosis during the ROS formation [37]. Accordingly, given the structure of THP aglycone metabolites retains the redox cycling anthraquinone moiety, it is likely that THP aglycone metabolites are biomarkers indicative of severe myocardial damage.

TCA cycle plays a key role in the pathway of sugar catabolism and energy production where it is a major source of adenosine triphosphate (ATPs) production. The pentose phosphate pathway, is another energy supply chain through the production of NADPH [39,40]. Accordingly, the significant decrease in the levels of citrate and D-glucuronic acid-1-phosphate after successive THP doses indicated that the activity of both TCA cycle and pentose pathway were compromised. A severely disturbed energy metabolic pathway will lead to a reduction in aerobic formation of ATP [26]. Generally, this will promote anaerobic ATP production by glycolysis. However, the decreased level of lactate suggests that THP treatment also severely disturbed glycolysis, as lactate is the end product of glycolysis [41]. In addition, the diminution in production of N-acetyl-DL-tryptophan and N-acetylglutamine after THP treatment is indicative of a decrease in fatty acid and amino acid synthesis associated with disturbance of the TCA. Therefore, we conclude that severe disturbance in energy production due to a diminution of key intermediary metabolic pathways is also a consequence of successive doses of THP. Interestingly, we found that F-THP was significantly more associated with a decreased expressions of citrate, D-glucuronic acid-1-phosphate, N-acetyl-DL-tryptophan, N-acetylglutamine and lactate. As a result, changes in the expression of these intermediary metabolites is not only indicative of the damage induced by THP but also supports the benefit of liposomal drug delivery system in the administration of THP. This conclusion correlated well to the histopathology observations

that L-THP is comparatively safe and the cumulative cardiotoxicity of THP can be alleviated when encapsulated into the liposomes. Our results therefore support the use of L-THP in successive doses of THP by reducing systemic effects on intermediary metabolism associated with energy production.

It might be questioned that whether L-THP can possess high therapeutic index while reducing the cumulative cardiotoxicity of THP. Interestingly, HCS results showed that L-THP was more cell damaging than F-THP, suggesting that the liposomal preparation enhances THP delivery and attendant toxicity to the A549 cancer cells. Accordingly, we could further concluded that the therapeutic index of THP against lung cancer can be improved when encapsulated into the liposomes, and further research is needed to define the efficacy of L-THP on the tumor-bearing animals.

In conclusion, this study shows that THP causes systemic or cardiac toxicity via a significant decrease in the intermediary metabolic pathways associated with the key energy production as demonstrated by a diminution of metabolites associated with the TCA cycle, glycolysis, pentose phosphate and amino acid synthesis pathways. In addition, the cardiotoxicity observed from histopathology studies can be attributed to the formation of THP aglycones associated with redox cycling, and are believed to generate mitochondrial damaging ROS species. Our study also predicts that the therapeutic index of THP against lung cancer can be improved when treated with L-THP. Generally, we can conclude that the cumulative cardiotoxicity of successive doses of THP can be ameliorated when encapsulated into liposomes. Since liposomal drug delivery system is frequently used in the anthracyclines for chemotherapy, this research can provide comprehensive insights and guidance for the safety assessment of liposomal drug delivery system.

Conflict of interest statement

None of the authors has any conflicts of interest to disclose.

Acknowledgments

This work was supported by grants from the Natural Science Foundation of China (81173516, 30801548), National Sci-Tech Major Special Item, China (2009ZX09502-009), Shanghai Science and Technology Committee, Shanghai, China (08QA14060), Shanghai Education Commission Leading Academic Discipline Project, Shanghai, China (J50302), Sci-Tech Innovation Item, Shanghai Education Committee (12ZZ124). We also want to thank Su, P. (Pharmaceutical Department, Jiangxi University of Traditional Chinese Medicine, Nanchang, China) for her kind assistance in the HCS experiments and Patterson, L. (Institute of Cancer Therapeutics, University of Bradford, West Yorkshire, UK) for helpful discussions and language polishments.

References

[1] S.B. Ai, J.L. Duan, X. Liu, S. Bock, Y. Tian, Z.B. Huang, Mol. Pharm. 4 (2011) 140–153.
[2] R.F. Battisti, Y.Q. Zhong, L.Y. Fang, S. Gibbs, J. Shen, J. Nadas, G.S. Zhang, D.X. Sun, Mol. Pharm. 4 (2007) 140–153.
[3] W.J. Cong, Q.F. Liu, Q.L. Liang, Y.M. Wang, G.A. Luo, Biophys. Chem. 143 (2009) 154–160.
[4] S. Ganta, M. Amiji, Mol. Pharm. 6 (2009) 928–939.
[5] G. Minotti, P. Menna, E. Salvatorelli, G. Cairo, A.L. Gianni, Pharmacol. Rev. 56 (2004) 185–229.
[6] E. Koh, Y. Ueda, T. Nakamura, A. Kobayashi, S. Katsuta, H. Takahashi, Pediatr. Res. 51 (2002) 256–259.
[7] T. Saito, Y. Kasai, A. Wakui, H. Furue, H. Majima, H. Nitani, T. Niijima, C. Takeda, O. Abe, Y. Koyama, Jpn. J. Cancer Chemother. 13 (1986) 1060–1069.
[8] K. Dhingra, D. Frye, R.A. Newman, R. Walters, R. Theriault, G. Fraschini, T. Smith, A. Buzdar, G.N. Hortobagyi, Clin. Cancer Res. 1 (1995) 691–697.
[9] N. Niitsu, J. Yamazaki, M. Nakayama, M. Umeda, Nippon Ronen Igakkai Zasshi 35 (1998) 358–362.
[10] A.D. Bangham, M.M. Standish, J.C. Watkins, J. Mol. Biol. 13 (1965) 238–252.
[11] P. Zagana, M. Haikou, E. Giannopoulou, P.V. Ioannou, S.G. Antimisiaris, Mol. Nutr. Food Res. 53 (2009) 592–599.
[12] R. Kuai, W.M. Yuan, Y. Qin, H.L. Chen, J. Tang, M.Q. Yuan, Z.R. Zhang, Q. He, Mol. Pharm. 7 (2010) 1816–1826.
[13] J.Z. Zheng, D. Jaffray, C. Allen, Mol. Pharm. 6 (2009) 571–580.
[14] W.J. Cong, Q.F. Liu, X. Chen, R. Gao, J. Lu, Y.M. Wang, G.A. Luo, Drug Dev. Ind. Pharm. 36 (2010) 1186–1194.
[15] K. Kawano, K. Takayama, T. Nagai, Y. Maitani, Int. J. Pharm. 252 (2003) 73–79.
[16] J.F. Maddox, J.P. Luyendyk, G.N. Cosma, A.P. Breau, R.H. Bible, G.G. Harrigan, R. Goodacre, P.E. Ganey, G.H. Cantor, G.L. Cockerell, R.A. Roth, Toxicol. Appl. Pharmacol. 212 (2006) 35–44.
[17] M. Sieber, D. Hoffmann, M. Adler, V.S. Vaidya, M. Clement, J.V. Boventre, N. Zidek, E. Rached, A. Amberg, J.J. Callanan, W. Dekant, A. Mally, Toxicol. Sci. 109 (2009) 336–349.
[18] L. Wei, P. Liao, H. Wu, X. Li, F. Pei, W. Li, J. Wu, Toxicol. Appl. Pharmacol. 234 (2009) 314–325.
[19] Y. Bao, T. Zhao, X. Wang, Y. Qiu, M. Su, W. Jia, W. Jia, J. Proteome Res. 8 (2009) 1623–1630.
[20] F. Zhang, Z. Jia, P. Gao, H. Kong, X. Li, J. Chen, Q. Yang, P. Yin, J. Wang, X. Lu, F. Li, Y. Wu, G. Xu, Talanta 79 (2009) 836–844.
[21] X. Lu, Z. Xiong, J. Li, S. Zheng, T. Huo, F. Li, Talanta 83 (2006) 700–708.
[22] I.D. Wilson, J.K. Nicholson, J. Castro-Perez, J.H. Granger, K.A. Johnson, B.W. Smith, R.S. Plumb, J. Proteome Res. 4 (2005) 591–598.
[23] G.X. Xie, X.J. Zheng, X. Qi, Y. Cao, Y. Chi, M. Su, Y. Ni, Y.P. Qiu, Y.M. Liu, H.K. Li, A.H. Zhao, W. Jia, J. Proteome Res. 9 (1) (2010) 125–133.
[24] V.C. Abraham, D.L. Towne, J.F. Waring, U. Warrior, D.J. Burns, J. Biomol. Screen. 13 (2008) 527–537.
[25] L.A.B. Rawlinson, P.J.O. Brien, D.J. Brayden, J. Control. Release 146 (2010) 84–92.
[26] X.P. Liang, X. Chen, Q.L. Liang, H.Y. Zhang, P. Hu, Y.M. Wang, G.A. Luo, J. Proteome Res. 10 (2011) 790–799.
[27] Z. Jiang, J. Sun, Q. Liang, Y. Cai, S. Li, Y. Huang, Y. Wang, G. Luo, Talanta 84 (2011), 298-234.
[28] X. Zheng, M. Su, L. Pei, T. Zhang, X. Ma, Y. Qiu, H. Xia, F. Wang, X. Zheng, X. Gu, X. Song, X. Li, X. Qi, G. Chen, Y. Bao, T. Chen, Y. Chi, A. Zhao, W. Jia, J. Proteome Res. 10 (2011) 4845–4854.
[29] Y. Qiu, G. Cai, M. Su, T. Lu, Y. Liu, Y. Xe, Y. Ni, A. Zhao, S. Cai, L. Xu, W. Jia, J. Proteome Res. 9 (2010) 1627–1634.
[30] C.A. Vivek, L.T. Danli, F.W. Jeffrey, W. Usha, J.B. David, J. Biomol. Screen. 13 (2008) 527–537.
[31] A. Mordente, E. Meucci, A. Silvestrini, G.E. Martorana, B. Giardina, Curr. Med. Chem. 16 (2009) 1656–1672.
[32] F.R. Leca, L.D. Marchise, A. Aleani, A. Noble, J. Catalin, Anti-cancer Drug 9 (1998) 503–509.
[33] Y. Matsushita, H. Iguchi, T. Kiyisaki, H. Tone, T. Ishikura, J. Antibiot. 36 (1983) 880–885.
[34] L.D. Marchise, F.R. Leca, A. Galeani, A. Noble, J. Catalin, Cancer Chemother. Pharmacol. 36 (1995) 239–243.
[35] L. Zhao, Y.M. Wei, X.D. Zhong, Y. Liang, X.M. Zhang, W. Li, B.B. Li, Y. Wang, Y. Yu, J. Pharm. Biomed. Anal. 49 (2009) 989–996.
[36] H. Haibach, M.W. Hosler, Cell Mol. Life Sci. 41 (1985) 39–40.
[37] L. Gille, H. Nohl, Free Radic. Biol. Med. 23 (1997) 775–782.
[38] P.M. Sokolove, Int. J. Biochem. 26 (1994) 1341–1350.
[39] W.C. Stanley, H.N. Sabbah, Heart Fail. Rev. 10 (2005) 275–279.
[40] W.C. Stanley, F.A. Recchia, G.D. Lopaschuk, Physiol. Rev. 85 (2005) 1093–1129.
[41] B.D. Guth, J.A. Wisneski, R.A. Neese, F.C. White, G. Heusch, C.D. Mazer, E.W. Gertz, Circulation 81 (1990) 1948–1958.